Biosensors and Bioelectronics 26 (2011) 3233–3239

Contents lists available at ScienceDirect

Biosensors and Bioelectronics

journal homepage: www.elsevier.com/locate/bios

Self-assembled monolayer-assisted silicon nanowire biosensor for detection of protein–DNA interactions in nuclear extracts from breast cancer cell

Guo-Jun Zhang [a,*], Min Joon Huang [a], Jun'An Jason Ang [a], Edison T. Liu [b], Kartiki Vasant Desai [b]

[a] Institute of Microelectronics, A*STAR (Agency for Science, Technology and Research), 11 Science Park Road, Singapore Science Park II, Singapore 117685, Singapore
[b] Genome Institute of Singapore, ASTAR (Agency for Science, Technology and Research), 60 Biopolis Street, Singapore 138672, Singapore

ARTICLE INFO

Article history:
Received 23 September 2010
Received in revised form 1 December 2010
Accepted 21 December 2010
Available online 28 December 2010

Keywords:
Silicon nanowire
Biosensor
Self-assembled monolayer
Interactions
Protein
DNA

ABSTRACT

The large number of estrogen receptor (ER) binding sites of various sequence patterns requires a sensitive detection to differentiate between subtle differences in ER–DNA binding affinities. A self-assembled monolayer (SAM)-assisted silicon nanowire (SiNW) biosensor for specific and highly sensitive detection of protein–DNA interactions, remarkably in nuclear extracts prepared from breast cancer cells, is presented. As a typical model, estrogen receptor element (ERE, dsDNA) and estrogen receptor alpha (ERα, protein) binding was adopted in the work. The SiNW surface was coated with a vinyl-terminated SAM, and the termination of the surface was changed to carboxylic acid via oxidation. DNA modified with amine group was subsequently immobilized on the SiNW surface. Protein–DNA binding was finally investigated by the functionalized SiNW biosensor. X-ray photoelectron spectroscopy (XPS) and atomic force microscopy (AFM) were employed to characterize the stepwise functionalization of the SAM and DNA on bare silicon surface, and to visualize protein–DNA binding on the SiNW surface, respectively. We observed that ERα had high sequence specificity to the SiNW biosensor which was functionalized with three different EREs including wild-type, mutant and scrambled DNA sequences. We also demonstrate that the specific DNA-functionalized SiNW biosensor was capable of detecting ERα as low as 10 fM. Impressively, the developed SiNW biosensor was able to detect ERα–DNA interactions in nuclear extracts from breast cancer cells. The SAM-assisted SiNW biosensor, as a label-free and highly sensitive tool, shows a potential in studying protein–DNA interactions.

1. Introduction

Over the last several years, silicon nanowire (SiNW) field-effect transistor (FET) based biosensor has emerged as a label-free and highly sensitive analytical assay. It allows for identification of a variety of analytes including metal ions (Zhang et al., 2007), nucleic acids (Bunimovich et al., 2006; Gao et al., 2007; Hahm and Lieber, 2004; Li et al., 2004; Zhang et al., 2008a,b, 2009, 2010a,b), protein (Chua et al., 2009; Cui et al., 2001; Ishikawa et al., 2009; Lin et al., 2010; Stern et al., 2007a; Zheng et al., 2005), virus (Patolsky et al., 2004) and neuronal signals (Patolsky et al., 2006). To immobilize the affinity receptor on the SiNW surface, covalent attachment is preferable, compared to electrostatic adsorption methodology. Although electrostatic adsorption for immobilization of biomolecules is effective in many applications, the binding efficiency is low if the surfaces are neutrally charged since biomolecules passively adsorb to surfaces through ionic interactions. Furthermore, the biomolecules immobilized via electrostatic adsorption are random in orientation and conformation, which further lowers the binding efficiency for the target molecules. Covalent immobilization is able to bind biomolecules through chemical bonds, which are specific, strong and stable. In addition, proper orientation and conformation can be controlled by selecting the self-assembled monolayers as functional surfaces. Covalent immobilization thus leads to better biomolecule activity, more ordered molecule conformation, less nonspecific adsorption, and greater stability. Well-known approaches for attachment of the receptors on the natural silicon oxide surface involve covalent binding of the receptors to the functionalized siloxane layers, most popularly 3-aminopropyltrimethoxysilane (APTES). However, the difficulties in using APTES lie in the potential hydrogen bonding interactions between the amine functionality and surface silanol groups as well as multiple reaction modes and difficulty in controlling silane layer structures caused by the three ethoxy groups. In general, there are two methods for forming the APTES layers on the surface, one is liquid-based, and the other is vapor-based. The liquid phase depositions of silanes are employed in most groups who use APTES for silanization. In this case, the APTES molecules can be packed in several layers because of self-polymerization of APTES in solution, which do not form self-assembled monolayer (SAM) as

* Corresponding author. Tel.: +65 6770 5390; fax: +65 6774 5754.
E-mail address: zhanggj@ime.a-star.edu.sg (G.-J. Zhang).

0956-5663/$ – see front matter © 2010 Elsevier B.V. All rights reserved.
doi:10.1016/j.bios.2010.12.032

reported by our previously published paper (Zhang et al., 2004), also by other group (Moon et al., 1996). However, if the APTES molecule is bound to the surface by chemical vapor deposition, a SAM can be formed (Haller, 1978).

SAM is an organic interface, and has several advantages such as ease of preparation, precision of surface control, and a spectrum of possible surface chemistries. Organic SAM formed on the silicon surface has intensively been developed for various applications. Many types of biomolecular nanopatterns have successfully been produced based on this organic/silicon interface (Zhang et al., 2004, 2005). It was also proven that the densely packed organic SAM as the gate insulator shows reduced leakage current density, which indicates the compatibility of these SAMs with semiconductor nano-FET device and their wide applications in nanometer-scale electronics (Collet and Vuillaume, 1998). In addition, Cattani-Scholz et al. showed that organophosphonate-based SiNW biosensor functionalized with peptide nucleic acid (PNA) could be used to detect DNA (Cattani-Scholz et al., 2008). The organophosphonate SAM is not only stable, but also elegant to bond biological system to native silicon oxide surface. The developed SiNW biosensor was thus used for DNA detection via PNA-DNA hybridization.

To study protein–DNA interactions, estrogen receptor element (ERE, dsDNA) and estrogen receptor alpha (ERα, protein) binding was adopted in the work as it is one of the most typical models. ERα regulates gene expression by directly binding itself to the specific ERE sequences. Several methods in common use like gel mobility assay (Loven et al., 2001; Yi et al., 2002), footprinting (Driscoll et al., 1996), for analyzing specific protein–DNA interactions are available. However, not only are these assays tedious and time-consuming, but also they require labeling. New methods developed recently like DNA microarray technology (Bulyk, 2006), AFM (Lyubchenko and Shlyakhtenko, 2009; Wicaksono et al., 2004) and SPR (Su et al., 2006; Teh et al., 2007) revealed remarkable progress in the analysis of protein–DNA interactions. Despite the significance of these techniques, the need for a new tool which is capable of characterizing protein–DNA binding with high sensitivity is still desirable. Moreover, a direct detection of the protein–DNA interactions in crude samples with high specificity will make the tool more intriguing and applicable.

FET-based biosensor is playing more and more important role. Different from the conventional FET sensor that has a thin film-type semiconductor structure as gate insulator, the sensing behavior of the SiNW sensor is enhanced because of the extremely small cross-sectional area of the SiNW. As a result, charge accumulation or depletion near the SiNW surface because of surface charge change gives rise to a change in the significant portion of the SiNW cross-sectional area. Therefore, using the SiNW-based sensor will remarkably increase the detection sensitivity compared to the conventional FET sensors. In this article, we have developed the SAM-assisted SiNW biosensor for study of protein–DNA interactions in nuclear extracts prepared from MCF-7 breast cancer cells. A vinyl-terminated SAM was functionalized on the SiNW biosensor surface. To make use of the SAM's inherent advantages, the forward DNA sequence in ERE was modified with an amine groups at its 5 end. After annealing, the dsDNA was covalently tethered to the SiNW surface after its termination changed from vinyl to carboxyl via oxidation. The formed SAM as a desirable interface will not only promote surface receptor conformational control for good accessibility of the target molecule binding, but also provide good passivation properties on the native silicon oxide. As a result, the specificity and high sensitivity of protein–DNA binding has been demonstrated by the SAM-assisted SiNW biosensor. More importantly, the sensor enabled the direct detection of protein–DNA interactions in nuclear extracts from breast cancer cells.

2. Experimental

2.1. Materials

Chemicals that were involved to create the SAM are tetradecyltrichlorosilane and bicyclohexyl from Sigma. To covalently attach the ERE onto this SAM, 1-ethyl-3-(3-dimethylaminopropyl)-carbodiimide (EDC) and *N*-hydroxysuccinimide (NHS) from Sigma were employed. O-(2-Aminoethyl)-O′-methylpolyethyleneglycol 750 (amino-PEG) was purchased from Fluka. For cell culture, Dulbecco's modified Eagle's medium was purchased from Invitrogen/Gibco, and Fetal Bovine Serum was from Hyclone. For protein separation, nitrocellulose membranes were bought from Biorad. AC-15 mouse monoclonal was also obtained from Sigma.

Three different 25 bp ERE sequences were selected as probes. The three ERE sequences (Sigma–Aldrich) are wild-type ERE (wt-ERE) which possesses perfect palindromic GGTCA half-sites, mutant ERE (mut-ERE) which possesses two base-pair mismatched; one at each half sites, and scrambled ERE sequence (non-ERE), which contains the same genetic makeup as consensus sequence but in scrambled form to keep the GC content similar. The forward sequence of the wt-ERE is 5′-H_2N-CAACTGGGTCATTCTGACCTAGAAG-3′; the forward sequence of the mut-ERE is 5′-H_2N-CAACTGGT***T***CATTCTGA***T***CTAGAAG-3′; and the forward sequence of the non-ERE is 5′-H_2N-CAACTGATCGGTTCCTCGATAGAAG-3′.

1 × PBS (Phosphate Buffer Saline) from Sigma–Aldrich containing 10 mM EDTA (pH 7.5) was used to anneal the ERE containing oligonucleotides. The target, human recombinant ERα (Invitrogen), with a stock concentration of 2016 pmol/ml was diluted with HEPES buffer (40 mM HEPES-KOH at pH 7.4 containing 10 mM $MgCl_2$, 2 mM DTT and 0.2% Triton X-100) to the required concentration.

2.2. Fabrication of SiNW biosensor

The SiNW biosensor was fabricated using the approach reported previously. (Zhang et al., 2010b). In brief, the SiNW sensor was produced by self-limiting oxidation process of silicon beams patterned using conventional deep UV photolithography, which is electrically addressable on an individual basis. The SiNWs were formed in an array format through conventional optical lithography, etching and oxidation, and thus are fully compatible with CMOS technology. The nanowire chip for bio-sensing fabricated in the work is designed with 36 clusters of 5 nanowires each. The SiNW arrays are 90 μm in length and 2 μm spacing in between two wires.

2.3. Formation of vinyl-terminated self-assembled monolayer on the SiNW surface

The schematic diagram of the SAM-assisted SiNW biosensor for studying protein–DNA interactions is illustrated in Fig. 1. ERα and ERE binding was adopted in the work because previous work demonstrated that ERα-ERE binding, as an example of protein–DNA complexes, has good affinity and high sequence specificity (Su et al., 2006). A SAM of vinyl group was formed on SiNW surface by immersing the chip in a solution of 0.01 M tetradecyltrichlorosilane in bicyclohexyl for 40 min (Fig. 1a). Following which, the SiNW were washed once with chloroform, twice with ethanol and blown dry.

2.4. Oxidation of self-assembled monolayer

Oxidation of the vinyl group to carboxylic group was achieved by placing the SiNW in a mixture of 0.5 mM $KMnO_4$, 19.5 mM $NaIO_4$ and 1.8 mM K_2CO_3 for 24 h (Fig. 1b). The SiNW was then rinsed with

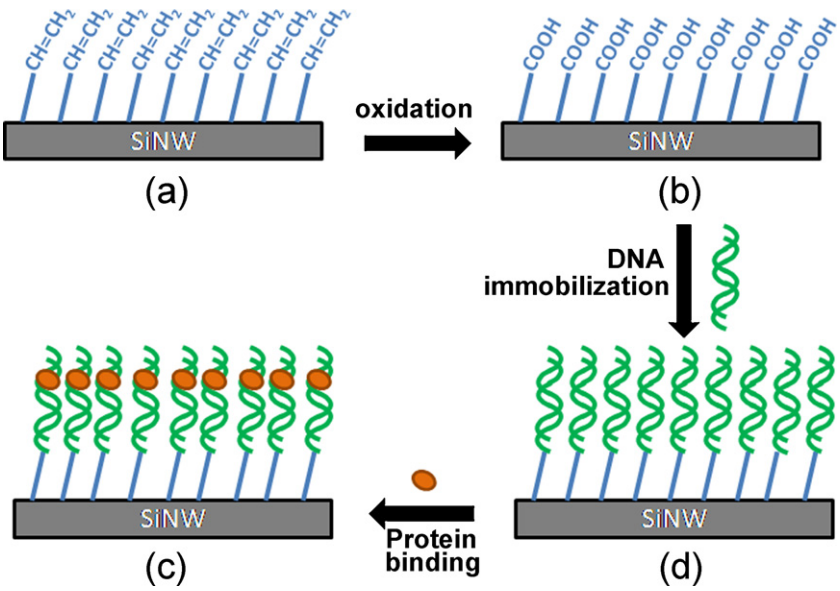

Fig. 1. Schematic diagram of a SAM-assisted SiNW biosensor for studying protein–DNA interactions. ERE is immobilized on the surface via a carboxyl-terminated SAM. Positively charged ER is bound to the specific ERE-functionalized SiNW biosensor, resulting in increase in conductance in the n-type SiNW biosensor.

a series of solutions, in the order of 0.3 M $NaHSO_4$, water, 0.1 M HCl, water and ethanol.

2.5. Immobilization of DNA on the SiNW surface

To covalently attach biomolecules onto carboxylic self-assembled surface, EDC-NHS offers a good linkage between the carboxylic groups and the amine-modified biomolecules. To achieve this, the SiNW was placed in a freshly prepared mixture of 0.2 M EDC and 0.05 M NHS for 30 min. The SiNW was washed with water to rinse away any excess EDC-NHS mixture. An acrylic well was adhered onto the SiNW chip to enclose the SiNW region. 10 μM of amine-modified ERE was then applied directly into the well and incubated in a moist environment for 2 h (Fig. 1c). Excess ERE was washed away with 1× PBS with 10 mM EDTA. To prevent non-specific binding of target, the ERE modified SiNW surface was then passivated with 1 mg/ml of amino-PEG.

2.6. Electrical measurement

To detect binding of ER to ERE modified surface, the conductance change of the SiNW is observed. Electrical measurements were taken in 10 μM HEPES buffer containing 1.5 mM KCl, 100 μM $MgCl_2$ and 10 μM EGTA (pH 7.4). The isoelectric point of ERα is approximately 8.3 while the pH of the buffer used is 7.4, hence ERα possesses a net positive charge. Binding of ERα to the ERE modified SiNW surface would induce a consequential increase in conductance because of the n-type SiNW. The sensor response refers to conductance change before and after protein bound to DNA immobilized on the SiNW surface. Directly after the application of the ERE probe on the SAM-assisted SiNW, 20 μl of 10 μM measuring HEPES buffer indicated above was added into the acrylic well before start of measurement. Thereafter, electrical measurements for 15 wires in conductance were taken using Alessi REL-6100 probe (Cascade Microtech, Beaverton) coupled with an Agilent 4156 parameter analyzer by probing the source (S) and drain (D) electrodes of the SiNW sensor. A single sweep of voltage was supplied to the source terminal in intervals of 0.05 V, with a compliance set at 100 mA, and subsequently the current was measured. After which, the measuring buffer was being rinsed away with ultra-pure water replaced with 20 μl of the ERα target. The ERα target was bound to the DNA molecules by incubation in a moist environment for 1 h (Fig. 1d). The unbounded ERα was washed away using HEPES buffer. Using the above-mentioned electrical measurement method, conductance for the same 15 wires was recorded again and the difference in conductance was analyzed using the formula, $[(G - G_o)/G_o] \times 100$.

2.7. X-ray photoelectron spectroscopy

X-ray photoelectron spectra were obtained on a PHI Quantera SXM Scanning X-ray Microprobe (ULVAC-PHI, Inc., Japan) using monochromatic Al Ka X-rays (1486.6 eV). Pass energy of 55 eV was used for high resolution (narrow) scan. The spot size was 200 μm. The sample surface was tilted at 45° with respect to the analyzer detector.

2.8. Atomic force microscope

AFM was carried out using a Dimension 5000 Scanning Probe Microscope (Veeco Instruments Inc., Plainview, NY). Topographic images were taken in tapping mode in air, collected at a scan rate of 1.5 Hz with a scan size of 1 μm.

2.9. Transfection of cells with siRNA and immunoblot analysis

MCF-7 (ER positive) and MDA MB231 (ER negative) breast cancer cells were maintained in Dulbecco's modified Eagle's medium supplemented with 10% Fetal Bovine Serum and maintained at 37 °C in a humidified atmosphere containing 5% CO_2. Reverse transfection protocol was carried out. Cells were transfected with predesigned short interfering RNA (siRNA) specific to ER (50 nmol) or scrambled control siRNA (75 nmol) as per manufacturer's instructions (ON-TARGETplus SMARTpool, Dharmacon) using 6×10^5 cells per well of a 6-well plate. Cell extracts from these transfected MCF7 and MDA MB 231 cells were prepared as described before (Su et al., 2008). To detect knockdown of ER protein in MCF7 cells, the lysates were separated by SDS-PAGE (10%) and transferred to nitrocellulose membranes. Immunoblotting was done using standard protocols. ER protein was detected using 1:1500 ERα (HC-20, rabbit polyclonal, Santa Cruz Biotechnology)

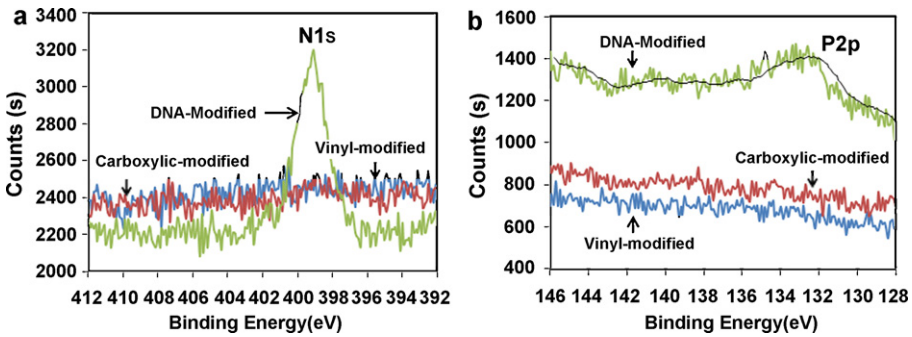

Fig. 2. XPS spectra of stepwise functionalization of SAM and DNA on the silicon surface. (a) Comparison of N 1s on the three various functionalized surfaces, the vinyl-modified surface, the carboxylic-modified surface, the DNA-modified surface, respectively, (b) Comparison of P 2p on the three various functionalized surfaces, the vinyl-modified surface, the carboxylic-modified surface, the DNA-modified surface, respectively.

and signals detected with an ECL+ Western Blotting Detection Kit (Amersham Bioscience). Protein loading was checked by reprobing the membranes with an anti-beta-actin antibody, 1:5000 dilution. Upon confirmation of ER knockdown, the lysates were used for ER binding assays.

3. Results and discussion

3.1. X-ray photoelectron spectroscopy characterization of DNA immobilization on the formed self-assembled monolayer

Prior to the sensing, the SiNW surface has to be immobilized with DNA via the functionalized SAM. The surface characterization of the stepwise functionalization was carried out on a bare silicon surface because the nanowire is too tiny to characterize. In this work, X-ray photoelectron spectroscopy (XPS) was used to characterize the resulting layers on the silicon surface. As described previously, bare Si(1 0 0) chip was cleaned and activated by oxidation (Zhang et al., 2010a). The prepared silicon surface was treated with the SAM of the vinyl-terminated carbon chain. Subsequent oxidation changed the termination of the SAM from vinyl to carboxyl. DNA was then immobilized on the silicon surface via amido between amine groups at the end of DNA and carboxyl groups on the silicon surface. Fig. S1 and Fig. 2 show XPS spectra for three elements: carbon (1s), nitrogen (1s) and phosphorous (2p) from the vinyl-terminated SAM, the carboxylic-terminated SAM and the DNA-modified surface, respectively. These three elements are able to differentiate the stepwise functionalization of the silicon surface, whereas the other two elements, Si 2p and O 1s, appear on each step of the chip functionalization and are not indicative. On the surface terminated with the vinyl SAM, the bulky C 1s was detected at 284.4 eV, contributed by combination of C–C and C=C bonds. In addition, the C 1s from Si–C bond was quite small, but the C 1s from C–O bond was still visible because of adsorption of water molecule on the surface (Fig. S1a). After oxidation, the vinyl groups were changed to the carboxylic acid by $KMnO_4$ and $NaIO_4$. As expected, the reaction replaces the $CH{=}CH_2$ group with a COOH group. In addition to the three C 1s abovementioned, another peak at 287.5 eV was obtained (Fig. S1b). This is attributed by the C=O bond from the COOH termination. The results are in good agreement with those reported previously by Whiteside group (Wasserman et al., 1989). An amido group was subsequently formed after DNA was immobilized, resulting in a C 1s peak at 288.0 eV (Fig. S1c). To further demonstrate that DNA has been successfully attached to the surface, two more elements, N 1s and P 2p, were compared from the three different surfaces. Obviously, neither N 1s nor P 2p were found from the Vinyl- and the carboxylic-terminated SAM surface. However, the N 1s shows a remarkable peak at 399.1 eV (Fig. 2a) and the P 2p shows a peak at 133.2 eV on the DNA-modified surface (Fig. 2b). The results reveal that the stepwise surface functionalization to build up the vinyl-terminated SAM, change the vinyl termination to the carboxylic acid, and immobilize DNA layer on the silicon surface is realized as anticipated.

3.2. Atomic force microscope illustration of protein–DNA binding on the SiNW surface

The immobilization of DNA on the SiNW surface was achieved by the methods above-mentioned. In order to investigate the protein–DNA binding on the SiNW surface, an atomic force microscope (AFM) was used to compare the morphology before and after binding of ERα to DNA. Fig. 3 shows representative AFM images of the SiNW, prior to the surface functionalization, after DNA immobilization and protein binding, respectively. The bare SiNW shows a clean and flat silicon surface with a negligible roughness over its length (Fig. 3a), whereas the DNA-modified SiNW surface indicates an uneven surface due to the DNA attached onto the SiNW surface (Fig. 3b). The height difference between the bare SiNW surface and the DNA-functionalized SiNW surface is estimated to be between 5 and 6 nm, which is consistent with the size of DNA. The DNA used in the work has 25 bp, and is ~8 nm in length if the DNA stands on the surface vertically. Considering the molecular size of DNA and the SAM on the surface, the height of DNA immobilized on the SiNW surface was thought to be in a reasonable region. Further functionalization of the SiNW with protein led to a height increase of ~6.6 nm (Fig. 3c). Because the diameter of the ERα is known to be several nanometers (approximately 67 kDa), the height was increased because of the formation of protein–DNA complex. To verify that ERα binds to the DNA-functionalized SiNW surface specifically rather than adsorption, a negative control was conducted, in which the SiNW surface was passivated with amino-PEG instead of DNA molecules after treatment with NHC-EDC. The PEG-functionalized SiNW surface then underwent AFM observation after it was incubated with ERα. It was observed that no adsorption of ERα molecule occurred on the passivated SiNW surface (data not shown). The data show that AFM, as a useful tool, has been utilized to demonstrate the molecular interactions between protein and DNA on the SiNW surface.

3.3. Specificity of protein–DNA binding

ERα is capable of distinguishing the wild-type, the mutant and the scrambled ERE, which was demonstrated by SPR-based biosensor (Su et al., 2006). The SPR-based sensor has emerged as a powerful technology to study protein–DNA interactions due to its ability of real-time measurement and the versatilities for studying affinity, kinetics, stoichiometry, sequence specificity, etc. Also,

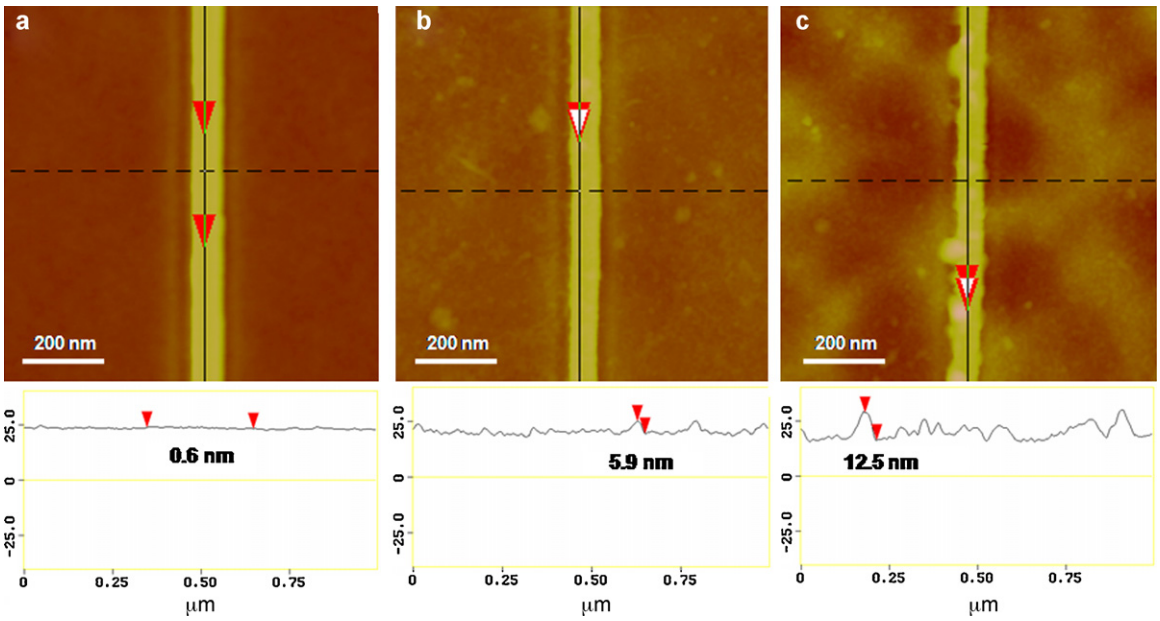

Fig. 3. AFM images of a typical SiNW (a) bare, (b) modified with DNA, and (c) bound with protein.

it is a quantitative analysis. Similar to the SPR-based sensor, the SiNW-based sensor is able to achieve real-time detection and distinguish sequence specificity. Differently, the nanoscale FET-based biosensor can give rise to higher sensitivity based on the scenario of the label-free electrical measurement.

To investigate whether the SAM-assisted SiNW biosensor is able to demonstrate the specificity of ERα-ERE binding, three different DNA sequences including wild-type, mutant, and non-specific, each of which was modified with amine group at its 5 end in the forward sequence, were immobilized on the SiNW surface via the formed SAM. As shown in Fig. 4, a ~33% conductance increase was obtained while ERα was applied to the wt-ERE-functionalized SiNW biosensor. A negligible change in conductance was observed while ERα was bound to the scrambled DNA-functionalized SiNW biosensor. Since the mutant DNA has two bases mutation in the palindromic GGTCA half-site, the binding between ERα and the mutant DNA is weaker than that of ERα and the wt-ERE, resulting in a smaller increase (~8.4%) in conductance. These results demonstrate that the SiNW biosensor is able to determine the sequence-dependent protein–DNA interactions, which is consistent with that achieved by SPR.

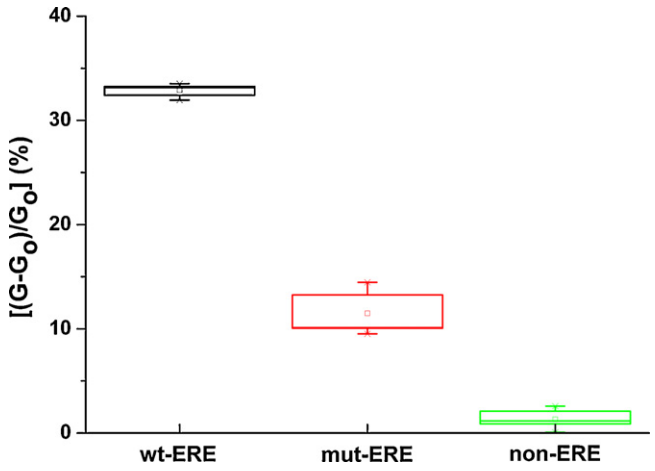

Fig. 4. Specificity of ERα with various EREs immobilized on the SAM-assisted SiNW biosensor surface.

3.4. Sensitivity

The SiNW biosensor has the advantages of label-free and sensitive detection of biomolecules. Many types of SiNW biosensors have been developed for various applications depending on the different fabrication process. The performance of the SiNW biosensor is affected by many aspects involving dimensions, carrier densities and mobilities, and choice of the surface chemistry, etc. It was found that smaller dimensions of the NWs resulted in a greater sensitivity (Stern et al., 2007b). This finding indicates the importance of NW fabrication of small dimension in order to achieve high levels of sensitivity. The SiNW generated by bottom-up approach has widely been used, however, the SiNW produced is random in orientation and varies in dimension, resulting in poor device uniformity and low fabrication yield. Top-down technologies use nanofabrication tools like e-beam lithography or photolithography to produce the SiNW. The resulting SiNW is uniform and well aligned. Our technology uses photolithography combined with self-limiting oxidation to fabricate the SiNW biosensor, which is CMOS compatible for manufacturability. Moreover, it shows potentials for integration with integrated circuits for miniaturization towards development of point-of-care device.

To demonstrate the limit of detection of the SAM-assisted SiNW biosensor, wt-ERE was immobilized on the SiNW surface and various known concentrations of ERα from 1 pM to 1 fM were applied to the specific DNA-functionalized SiNW surface. Fig. 5 shows ERα concentration-dependent response to the wt-ERE-functionalized SiNW biosensor. The response reduces along with the diluted concentrations of ERα. Almost negligible response was found when 1 fM ERα was bound to the DNA. On the contrary, 1 pM ERα bound to the surface gave rise to a ~33% increase in conductance. Moreover, a ~10.3% conductance increase was obtained when 10 fM ERα was used. The data shown indicate that the wild-type DNA-functionalized SiNW biosensor can achieve LOD as low as 10 fM, which are 3 orders of magnitude lower than that obtained by SPR-based biosensor (Su et al., 2006).

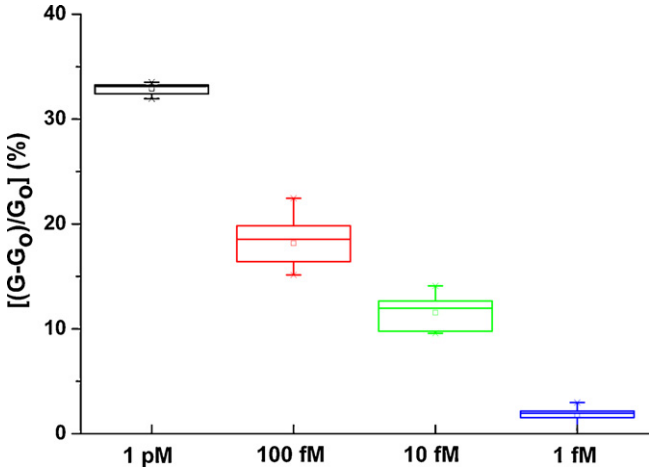

Fig. 5. Response of the wt-ERE-functionalized SiNW biosensor to various concentrations of specific ERα.

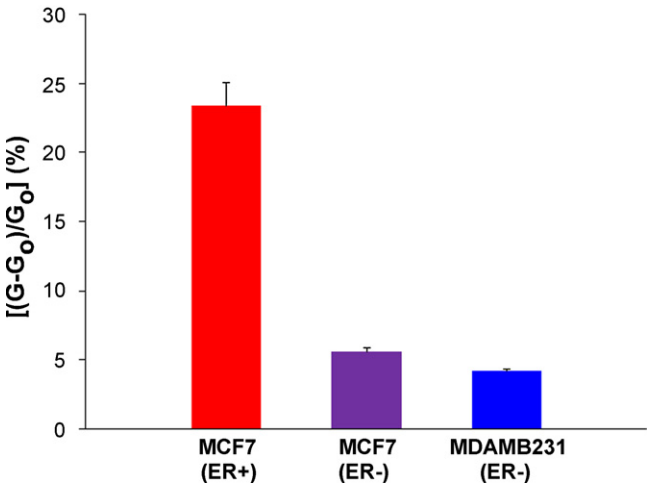

Fig. 6. Response of the wt-ERE-functionalized SiNW biosensor to the nuclear extracts from MCF-7 and MDA MB231 breast cancer cells.

3.5. Direct detection of protein–DNA interactions in nuclear extracts from MCF-7 breast cancer cells

Direct detection of protein–DNA binding in biological samples, in most cases, is quite difficult mainly because the amount of the protein to be detected is insufficient and the samples are impure. Hence the sample preparation for protein purification is important in protein assay. On one side, protein purification is very important for analysis, which is capable of minimizing the interference of other impurities in the crude extract. On the other side, some degree of product loss takes place during each protein purification step. Therefore, the strategy for protein purification is that the highest level of purification is obtained in the fewest steps. To purify intracellular proteins, a crude extract containing a complex mixture of all the proteins from the cell cytoplasm, and some additional macromolecules, cofactors and nutrients is prepared. The preparation of the crude protein extracts is carried out by removing cellular debris by centrifugation and recovering the supernatant. Main techniques for protein purification include chromatography and electrophoresis.

To amplify the signal for detection of the binding of native ERα from human mammary carcinoma cell extracts to its DNA response element, a two-step antibody approach has been developed (Su et al., 2008). A couple of antibodies involving rabbit anti-ERα and goat anti-rabbit IgG were used for binding after the nuclear extracts were bound to the surface-immobilized DNA. Although the method improved sensitivity through the amplification, it involved multiple additional steps, thus was not direct.

Owing to the high sensitivity that SiNW biosensor confers, a direct detection method for studying protein–DNA interactions in nuclear extracts from breast cancer cells was investigated. Extracts from 2 breast cancer cell lines, MCF-7, that is positive for ER expression (ER+) and MDA MB231 that does not express nor shows detectable ER protein (ER−) were used. To further evaluate the specificity of the detection in the impure sample, ERα was knocked down by siRNA in MCF-7 breast cancer cell. Fig. 6 shows the response of the wt-ERE-functionalized SiNW biosensor to the nuclear extracts from MCF-7 and MDA MB231 breast cancer cells. As seen, a remarkable conductance change (∼23.4%) was obtained when ERα in nuclear extracts was bound to the wt-ERE immobilized on the SiNW surface. ERα knocked down by siRNA in the same cell line and negative ERα from another cell line (MDA MB 231) gave rise to negligible response, ∼5.6% and ∼4.3%, respectively. The results demonstrate the capability of the SiNW biosensor for the versatile applications, in particular the direct detection of protein–DNA interactions in the complex environments of the real sample, which will shed light on ER-mediated gene expression for breast cancer.

4. Conclusion

We demonstrated a SAM-assisted SiNW biosensor for specific and highly sensitive characterization of protein–DNA interactions. The technique described here enables the direct detection of protein–DNA interactions in nuclear extracts from breast cancer cells without introducing other additional antibodies. The successful formation of the SAM and the immobilization of the DNA layer on the SiNW surface ensure the high affinity of protein–DNA binding. The SAM-assisted SiNW biosensor not only shows good sequence specificity between ERα and various EREs, but also achieves a high sensitivity. This protocol provides a successful demonstration of the monolayer-assisted SiNW biosensor for studying protein–DNA interactions, especially in nuclear extracts from breast cancer cells. Future work will be directed to the multiplexed characterization of protein–DNA interactions, which will assist the high resolution system to differentiate subtle differences in protein–DNA binding affinities.

Acknowledgments

The authors would like to acknowledge The Agency for Science, Technology and Research (A*STAR), Singapore, for the financial support under the grant CCOG01-005-2008.

The authors thank Ms. Dao Thuy Khanh Linh Kathy at Data Storage Institute in Singapore for her assistance with XPS spectra. We also thank Ms. Li Wei Hong Catherine at Institute of Microelectronics for her help with AFM observation.

Appendix A. Supplementary data

Supplementary data associated with this article can be found, in the online version, at doi:10.1016/j.bios.2010.12.032.

References

Bulyk, M.L., 2006. Curr. Opin. Biotechnol. 17, 422–430.
Bunimovich, Y.L., Shin, Y.S., Yeo, W.-S., Amori, M., Kwong, G., Heath, J.R., 2006. J. Am. Chem. Soc. 128, 16323–16331.
Cattani-Scholz, A., Pedone, D., Dubey, M., Neppl, S., Nickel, B., Feulner, P., Schwartz, J., Abstreiter, G., Tornow, M., 2008. ACS Nano 2, 1653–1660.
Collet, J., Vuillaume, D., 1998. Appl. Phys. Lett. 73, 2681–2683.

Chua, J., Chee, R.E., Agarwal, A., Wong, S.M., Zhang, G.-J., 2009. Anal. Chem. 81, 6266–6271.
Cui, Y., Wei, Q.Q., Park, H.K., Lieber, C.M., 2001. Science 293, 1289–1292.
Driscoll, M.D., Klinge, C.M., Hilf, R., Bambara, R.A., 1996. J. Steroid Biochem. Mol. Biol. 58, 45–61.
Gao, Z.-Q., Agarwal, A., Trigg, A.D., Singh, N., Fang, C., Tung, C.-H., Fan, Y., Buddharaju, K.D., Kong, J.-M., 2007. Anal. Chem. 79, 3291–3297.
Hahm, J.-I., Lieber, C.M., 2004. Nano Lett. 4, 51–54.
Haller, I., 1978. J. Am. Chem. Soc. 100, 8050–8055.
Ishikawa, F.N., Chang, H.-K., Curreli, M., Liao, H.-I., Olson, C.A., Chen, P.C., Zhang, R., Roberts, R.W., Sun, R., Cote, R.J., Thompson, M.E., Zhou, C., 2009. ACS Nano 3, 1219–1224.
Li, Z., Chen, Y., Li, X., Kamins, T.I., Nauka, K., Williams, R.S., 2004. Nano Lett. 4, 245–247.
Lin, T.-W., Hsieh, P.-J., Lin, C.-L., Fang, Y.-Y., Yang, J.-X., Tsai, C.-C., Chiang, P.-L., Pan, C.-Y., Chen, Y.-T., 2010. Proc. Natl. Acad. Sci. U. S. A. 107, 1047–1052.
Loven, M.A., Wood, J.R., Nardulli, A.M., 2001. Mol. Cell Endocrinol. 181, 151–163.
Lyubchenko, Y.L., Shlyakhtenko, L.S., 2009. Methods 47, 206–213.
Moon, J.H., Shin, J.W., Kim, S.Y., Park, J.W., 1996. Langmuir 12, 4621–4624.
Patolsky, F., Timko, B.P., Yu, G., Fang, Y., Greytak, A.B., Zheng, G., Lieber, C.M., 2006. Science 313, 1100–1104.
Patolsky, F., Zheng, G., Hayden, O., Lakadamyali, M., Zhuang, X., Lieber, C.M., 2004. Proc. Natl. Acad. Sci. U. S. A. 101, 14017–14022.
Stern, E., Klemic, J.F., Routenberg, D.A., Wyremebak, P.N., Turner-Evans, D.B., Hamilton, A.D., LaVan, D.A., Fahmy, T.M., Reed, M.A., 2007a. Nature 445, 519–522.
Stern, E., Wagner, R., Sigworth, F.J., Breaker, R., Fahmy, T.M., Reed, M.A., 2007b. Nano Lett. 7, 3405–3409.
Su, X.D., Lin, C.Y., O'Shea, S.J., Teh, H.F., Peh, W.Y.X., Thomsen, J.S., 2006. Anal. Chem. 78, 5552–5558.
Su, X.D., Neo, S.J., Peh, W.Y.X., Thomsen, J.S., 2008. Anal. Biochem. 376, 137–143.
Teh, H.F., Peh, W.Y.X., Su, X.D., Thomsen, J.S., 2007. Biochemistry 46, 2127–2135.
Wasserman, S.R., Tao, Y.T., Whitesides, G.M., 1989. Langmuir 5, 1074–1087.
Wicaksono, D.H.B., Ebihara, T., Funabashi, H., Mie, M., Yanagida, Y., Aizawa, M., Kobatake, E., 2004. Biosens. Bioelectron. 19, 1573–1579.
Yi, P., Driscoll, M.D., Huang, J., Bhagat, S., Hilf, R., Bambara, R.A., Muyan, M., 2002. Mol. Endocrinol. 16, 674–693.
Zhang, G.-J., Agarwal, A., Buddharaju, K.D., Singh, N., Gao, Z.-Q., 2007. Appl. Phys. Lett. 90, 233903–233905.
Zhang, G.-J., Chua, J., Chee, R.E., Agarwal, A., Wong, S.M., 2009. Biosens. Bioelectron. 24, 2504–2508.
Zhang, G.-J., Chua, J., Chee, R.E., Agarwal, A., Wong, S.M., Buddharaju, K.D., Balasubramanian, N., 2008a. Biosens. Bioelectron. 23, 1701–1707.
Zhang, G.-J., Luo, Z.H.H., Huang, M.J., Tay, G.K.I., Lim, E.-J.A., 2010a. Biosens. Bioelectron. 25, 2447–2453.
Zhang, G.-J., Tanii, T., Funatsu, T., Ohdomari, I., 2004. Chem. Commun., 786–787.
Zhang, G.-J., Tanii, T., Zako, T., Hosaka, T., Miyake, T., kanari, Y., Funatsu, T., Ohdomari, I., 2005. Small 1, 833–837.
Zhang, G.-J., Zhang, G., Chua, J., Chee, R.E., Wong, E.H., Agarwal, A., Buddharaju, K.D., Singh, N., Gao, Z.Q., Balasubramanian, N., 2008b. Nano Lett. 8, 1066–1070.
Zhang, G.-J., Zhang, L., Huang, M.J., Luo, Z.H.H., Tay, G.K.I., Lim, E.-J.A., Kang, T.G., Chen, Y., 2010b. Sens. Actuators B: Chem. 146, 138–144.
Zheng, G., Patolsky, F., Cui, Y., Wang, W.U., Lieber, C.M., 2005. Nat. Biotechnol. 23, 1294–1301.